Gut microbial metabolomics to understand allergies in early life

Savova, M.V.

Chapter 4

Exploring the fecal metabolome in infants with cow's milk allergy: The distinct impacts of cow's milk protein tolerance acquisition and of synbiotic supplementation

Based on:

Exploring the fecal metabolome in infants with cow's milk allergy: The distinct impacts of cow's milk protein tolerance acquisition and of synbiotic supplementation

Pingping Zhu[1,#], **Mariyana V. Savova[1,#]**, Alida Kindt[1], the PRESTO study team, Harm Wopereis[2], Clara Belzer[3], Amy C. Harms[1], Thomas Hankemeier[1]

Molecular Nutrition & Food Research **69**, e202400583 (2025)
DOI: 10.1002/mnfr.202400583

[#]authors contributed equally

Abstract

Scope: Cow's milk allergy (CMA) is one of the most prevalent food allergies in early childhood, often treated via elimination diets including standard amino acid-based formula or amino acid-based formula supplemented with synbiotic (AAF or AAF-S). This work aimed to assess the effect of cow's milk (CM) tolerance acquisition and synbiotic (inulin, oligofructose, *Bifidobacterium breve* M-16 V) supplementation on the fecal metabolome in infants with IgE-mediated CMA.

Methods and Results: The CMA-allergic infants received AAF or AAF-S for a year during which fecal samples were collected. The samples were subjected to metabolomics analyses covering gut microbial metabolites including SCFAs, tryptophan metabolites, and bile acids (BAs). Longitudinal data analysis suggested amino acids, BAs, and branched SCFAs alterations in infants who outgrew CMA during the intervention. Synbiotic supplementation significantly modified the fecal metabolome after 6 months of intervention, including altered purine, BA, and unsaturated fatty acid levels, and increased metabolites of infant-type *Bifidobacterium* species: indolelactic acid and 4-hydroxyphenyllactic acid.

Conclusion: This study offers no clear conclusion on the impact of CM-tolerance acquisition on the fecal metabolome. However, our results show that 6 months of synbiotic supplementation successfully altered fecal metabolome and suggest induced bifidobacteria activity, which subsequently declined after 12 months of intervention.

Keywords

early life, metabolomics, food allergy, bifidobacteria, fructooligosaccharides

Abbreviations

AAF: amino acid-based formula; **AAF-S**: amino acid-based formula with synbiotic; **BSCFA**: branched short-chain fatty acid; **BSH**: bile salt hydrolase; **CI**: confidence interval; **CM**: cow's milk; **CMA**: cow's milk allergy; **DBPCFC**: double-blind, placebo-controlled food challenge; **FOS**: fructooligosaccharide(s); **GM**: gut microbiome; **HMO**: human milk oligosaccharide; **IgE**: immunoglobin E; **LMM**: linear mixed model; **QC**: quality control; **RM-ASCA+**: repeated measures analysis of variance simultaneous component analysis+; **SCORAD**: SCORing Atopic Dermatitis; **T_{reg}**: regulatory T cell

1. Introduction

Cow's milk allergy (CMA), characterized by an immune-mediated response to cow's milk protein(s), is one of the major food allergies in early life.[1,2] Over the past decades, the estimated CMA prevalence in children of developed countries is approximately 0.5%–3%.[3,4] The allergic symptoms typically occur in the first year of life, whereas the resolution age varies and is related to the type of CMA.[5] Based on symptoms and pathophysiology, CMA is categorized into immunoglobin E (IgE)-mediated, non-IgE mediated, and mixed IgE CMA.[6] Subjects with IgE-mediated CMA, constituting approximately 60% of all CMA cases,[3] require longer time for tolerance acquisition to CM than non-IgE mediated CMA subjects.[7,8] In recent decades, the relevance of the gut microbiome (GM) in CMA has been highlighted, and studies show that compared to healthy counterparts, children with IgE-mediated CMA exhibit a reduction in bifidobacteria.[9]

Bifidobacteria, the prototypical health-promoting bacteria, are dominant inhabitants in a breast-fed infant's gut[10] and play a pivotal role in GM development in early life.[11,12] As coevolved bacteria, bifidobacteria possess unique glycosidases to digest complex host-derived glycans, particularly the human milk oligosaccharides (HMOs).[13,14] The oligosaccharide fermentation products not only satisfy the energy and carbon demands of bifidobacteria but also benefit other bacteria through cross-feeding activities, thereby contributing to maintaining the GM homeostasis in early life.[10,11]

Thus, bifidobacteria-related probiotics and HMO-mimicked prebiotics have gained popularity in the management of CMA in early life, alongside the conventional interventions with extensively hydrolyzed formula or amino acid-based formula (AAF).[15] Indigestible oligosaccharides, such as fructooligosaccharides (FOS) and galactooligosaccharides, are used as prebiotics due to their bifidogenic effect on the GM.[16] Bifidobacterium species, including *B. bifidum*,[17] *B. longum*,[18] and particularly *B. breve*,[18–21] are widely used probiotics for IgE-mediated CMA management in infants. These bifidobacteria have key immunomodulatory roles in the cross-talk between GM and host immune system: *B. bifidum*, for example, can induce the expression of FoxP3 in the regulatory T (Treg) cells through cell surface polysaccharides,[22] while B. longum in neonatal microbiota can alleviate the risk of allergy by promoting the Treg maturation;[23] *B. breve*, particularly the *B. breve* M-16V, can trigger the antiallergic process in early infancy by regulating the intestinal microbiota, intestinal epithelial barrier, and immune system.[24] Overall, bifidobacteria with HMO-utilization genes are found to induce intestinal IFN-β and silence Th2 and Th17 cytokines, thereby regulating the systemic immune balance in infants.[25] Additionally, by breaking down HMOs, bifidobacteria can indirectly enhance the production of butyrate[26] which is essential for the interplay between GM and systemic immunity,[27] possibly through epigenetic mechanisms.[28] Bifidobacteria-derived indolelactic acid (ILA) also actively engages in the immunoregulation during infancy.[25,29] However, despite these findings and the wide application of bifidobacteria-related interventions for IgE-mediated CMA,[17–21] none of the studies have reported comprehensive metabolome exploration.

In this study, we investigated longitudinal fecal metabolome changes of infants with IgE-mediated CMA undergoing dietary management with AAF, with and without synbiotic (*B. breve* M-16V; FOS: oligofructose, inulin). By applying linear mixed models (LMMs) and repeated measures analysis of variance simultaneous component analysis+ (RM-ASCA+), we compared the longitudinal fecal metabolome of infants with persistent CMA to those who developed CM-tolerance and identified key metabolic changes, associated with the synbiotic intervention.

2. Experimental section

2.1 Study design and dosage information

This study arises from a multicenter, randomized, double-blind, controlled clinical study PRESTO (registered as NTR3725 in Netherlands Trial Register). Detailed information on ethics committees, institutional review boards, and regulatory authorities that approved the study was previously published.[30]

PRESTO enrolled infants diagnosed with IgE-mediated CMA who then received either AAF (Nutricia, Liverpool, UK) or amino acid-based formula with synbiotic (AAF-S) to manage their CMA. The synbiotic blend consisted of chicory-derived neutral FOS: oligofructose and inulin in a 9:1 ratio (total concentration of 0.63g/100 mL formula, BENEO-Orafti SA, Oreye, Belgium) and *B. breve* M-16V (1.47×10^9 cfu/100 mL formula, Morinaga Milk Industry, Tokyo, Japan). Caretakers were instructed to provide subjects with a minimum daily dose of 450mL, 350mL, and 250mL for infants aged 0 to 8 months, 9 to 18 months, and older than 18 months, respectively.[19] After 12 months of intervention, the allergy status was re-evaluated through double-blind, placebo-controlled food challenge (DBPCFC) with CM. Detailed information on the diagnosis and reassessment was previously published.[19] Out of the 169 participants enrolled in PRESTO, 40 subjects (aged 3-13 months) were selected for this study based on sample availability. One subject was excluded due to unclear allergy status after 12 months.[30] Of the 16 AAF and 23 AAF-S participants, 10 and 14 infants, respectively, outgrew CMA within 12 months. Stool samples were available at 0 (baseline, TP0), 6 (TP1), and 12 months (TP2) after the start of the intervention, resulting in a total of 117 samples.

2.2 Sample collection and storage

The sample collection procedure has been described previously.[30] In short, fecal samples were collected at home and immediately stored in freezers, then transferred on ice to the participant hospitals and stored at -80°C until transfer to Danone Research & Innovation (Utrecht, the Netherlands) for wet sample aliquoting and SCFAs and lactic acid analysis. Sample aliquots for LC-MS metabolomics analysis were transferred on dry-ice to Leiden University and stored at -80°C until analysis.

2.3 Metabolomic analysis

2.3.1 SCFAs and lactic acid analysis

Quantitative SCFAs, including branched SCFAs (BSCFAs) analysis was performed using GC coupled to flame ionization detector and lactic acid was measured using lactic acid assay kit (Megazyme, Wicklow, Ireland) as previously described.[31]

2.3.2 LC-MS metabolomics analysis

The wet sample aliquots were lyophilized at 4 mbar and -110°C for 20h (Martin Christ Gefriertrocknungsanlagen GmbH, Germany), weighed (20±0.2mg), and stored at -80°C until extraction. Liquid-liquid extraction was performed as described by Hosseinkhani *et al.*[32] with adjusted sample amount and doubled solvent-to-feces ratio. Detailed information on the chemicals, the sample preparation, and the quality control (QC) is available in Supplementary Materials.

Polar to semi-polar metabolites, including acetylcarnitines, amines, benzenoids, organic acids, indoles, nucleosides, and nucleotides, were analyzed using reverse phase LC coupled with quadrupole (Q)-TOF-MS operated in full-scan positive and negative ionization modes, as described previously[33] and in the Supplementary Materials. Bile and fatty acids were measured using reverse phase LC separation using Q-TOF-MS operated in full scan negative ionization mode, as described in the Supplementary Materials.

Targeted peak integration was performed using SCIEX OS (version 2.1.6., SCIEX) with a maximum mass error of 10 ppm. The retention times were verified against authentic standards. In case of coelution, the targets were reported using the name or abbreviation of one of the targets followed by a "#". Details on the abbreviations used are listed in **Table S1** in Supplementary materials. For the polar to semi-polar metabolites, peak area was used for further data analysis, whereas for the bile and fatty acids, the area ratio of compounds to stable isotopically labeled standards (**Table S1** in Online Supplementary Materials) was used. Data quality inspection was performed using an in-house quality assurance software performing between batch correction and removal of metabolites with high technical variance (RSD of QC>30%).

2.3.3 Data analysis

Data handling and statistical analyses were performed in R (version 4.3.2). Metabolites with missingness above 20% and with median signal of the samples less than five times the mean signal of the procedure blanks were removed, leaving 166 metabolites. To identify group bias in missingness, Fisher's exact test was performed for metabolites with missingness above 20% at each time point after grouping the subjects by intervention or CM-tolerance status, and the results are summarized in **Table S2** in Online Supplementary Materials. Ratios of secondary to primary and unconjugated to conjugated bile acids (BAs) were added, resulting in a total of 177 variables. A list of the reported metabolites and their

abbreviations can be found in **Table S1**. The raw data were normalized by dry weight and subsequently log2-transformed. Missing values were imputed per metabolite using the quantile regression imputation of left-censored (QRILC) method.[34] Available clinical characteristics that potentially associated with CM-tolerance status at TP2 or intervention were analyzed with the two-sided Mann-Whitney U-test for numeric variables and the Fisher's exact test for binary variables as reported previously.[30,35]

To assess the change from TP0 to TP1 and TP2, LMMs were built using the lme4 package in R. Before building the model, the data was scaled by the standard deviation of all baseline samples. The metabolites were modelled as response variables with group and time as fixed effects and subject ID as a random effect. After grouping the subject by either their CM-tolerance status at TP2 (CM-allergic versus CM-tolerant) or intervention (AAF versus AAF-S), two models were built, namely tolerance-allergy and intervention. For the tolerance-allergy model (Metabolite ~ time + CM-tolerance_status + time:CM-tolerance_status + (1|ID)), TP0 and the CM-allergic group were used as references. Pairwise comparisons between groups at each time point and within a group between the time points were performed using the emmeans package in R. For the intervention model (Metabolite ~ time + time:intervention + (1|ID)), TP0 and the AAF group were used as references. The main effect of the intervention was removed from the model but its interaction with time was kept ensuring the groups are equal at baseline. The p values were calculated to assess a change from baseline with the Satterthwaite's degrees of freedom method using the lmerTest package within the ALASCA package.[36] In this study, the combined CM-tolerance status–intervention model was not performed because CM-tolerance acquisition as investigated in the parent study did not differ between the interventions at TP2 and aligned with natural rates of CMA outgrowth in infants.[19] For most metabolites, the addition of age as a covariate to models led to no improvement of the performance based on akaike information criterion (**Tables S4**-**S5** in Online Supplementary Materials). Therefore, age was not used as a covariate in the LMMs. Multiple testing correction was performed using the Benjamini-Hochberg method where Q<0.1 was considered as statistically significant.

Visualization of the longitudinal metabolomic alterations was achieved using RM-ASCA+ with ALASCA package,[36] as detailed in the Supplementary Materials. Performances of the analysis were validated using nonparametric bootstrapping, and the 95% confidence intervals (CI) were estimated based on 1000 resampling iterations.

2.4 16S rRNA gene sequencing and pre-processing

Extraction of DNA from stool samples and the subsequent gut microbiota profiling by 16S rRNA gene sequencing was performed as described previously.[30] Correlations between the changes in metabolites and the relative abundance of Bifidobacterium were examined using Spearman's rank correlation analysis. Relative abundance comparisons of Bifidobacterium between and within the AAF and AAF-S groups were evaluated with two-sided unpaired t-tests.

3. Results

3.1 Patient Characteristics

The statistical results of important clinical characteristics are summarized in **Tables S6-S7** in Online Supplementary Materials. When grouping the subjects by the CM-tolerance status at TP2, the father allergy occurrence and the SCORing Atopic Dermatitis (SCORAD) at baseline were significantly higher in the CM-allergic group than in the CM-tolerant group (**Table S6** in Online Supplementary Materials). None of the clinical characteristics were significantly different between AAF and AAF-S groups (**Table S7** in Online Supplementary Materials).

3.2 More pronounced fecal metabolome changes in the CM-tolerant group

Firstly, RM-ASCA+ was used to examine the longitudinal metabolome alterations within and between infants that remained allergic and those that acquired tolerance to CM by TP2 (CM-allergic vs. CM-tolerant). The PC1 score plot (**Figure 1A**) describes the direction of maximum variance in the modeled data, whereas the loadings plot (**Figure 1B**) highlights the top metabolites contributing to PC1. Metabolites with positive loadings follow the trend described by the score, whereas the opposite holds for metabolites with negative loadings. **Figure 1B** shows that almost half of the variation (47%) described by the fixed effects of the tolerance-allergy model was explained by PC1 (**Figure 1A**). The scores and loading for PC1 showed that over time ferulic acid, desaminotyrosine, pipecolic acid, 3-hydroxybenzoic acid increased, whereas dodecanoylcarnitine, pregnenolone sulfate, betaine, pyruvate decreased (**Figure 1**). Few BAs also showed overall change with time. The primary BAs cholic acid (CA), chenodeoxycholic acid (CDCA), and hyocholic acid (HCA) declined over time. In contrast, the secondary BAs deoxycholic acid (DCA) and the ratios of secondary to primary BAs, including DCA/CA, lithocholic acid (LCA)/CDCA, increased. Although with overlapped CIs between the two groups, those changes were more pronounced for the CM-tolerant group where the PC1 score declined more sharply than the CM-allergy group and for which the CI between the time points were separated, suggesting a significant time effect in this group.

Univariate marginal means comparison showed that around five times more metabolites were significantly altered over time in infants that acquired CM-tolerance versus those that remained CM-allergic (TP0-TP1: 9 metabolites in CM-tolerant vs. 2 metabolites in CM-allergic; TP0-TP2: 30 metabolites in CM-tolerant and 7 in CM-allergic; **Figure S1** and **Table S2**). Pregnenolone sulfate, pyroglutamic acid, pyruvate, oxoglutaric acid, and ferulic acid were significantly affected by time for both groups and followed comparable time-development trends (**Figure S1**). Similarly, arginine decreased, whereas 3-hydroxybenzoic acid, hydrocinnamic acid, LCA, DCA increased simultaneously in both groups, but significantly only in the CM-tolerant group (**Figure S1**). Pipecolic acid levels increased over time in both groups, but the rise was steeper and significant only in the CM-tolerant group.

Dodecanoylcarnitine followed the trend described by PC1 of the combined effect matrix (**Figure 1A**) with a decline in time at both TP1 and TP2 significant only in the CM-tolerant group. The rest of the significantly altered metabolites showed dissimilar longitudinal profiles between the groups (**Figure S1**). Butyric acid, PLA#, desaminotyrosine, and phenylacetic acid were significantly increased, whereas 5-hydroxytryptophan and the primary BAs CA and CDCA showed significant decreases in the CM-tolerant group only. In contrast, threonine#, and tryptophan significantly increased over time only in the CM-allergic group.

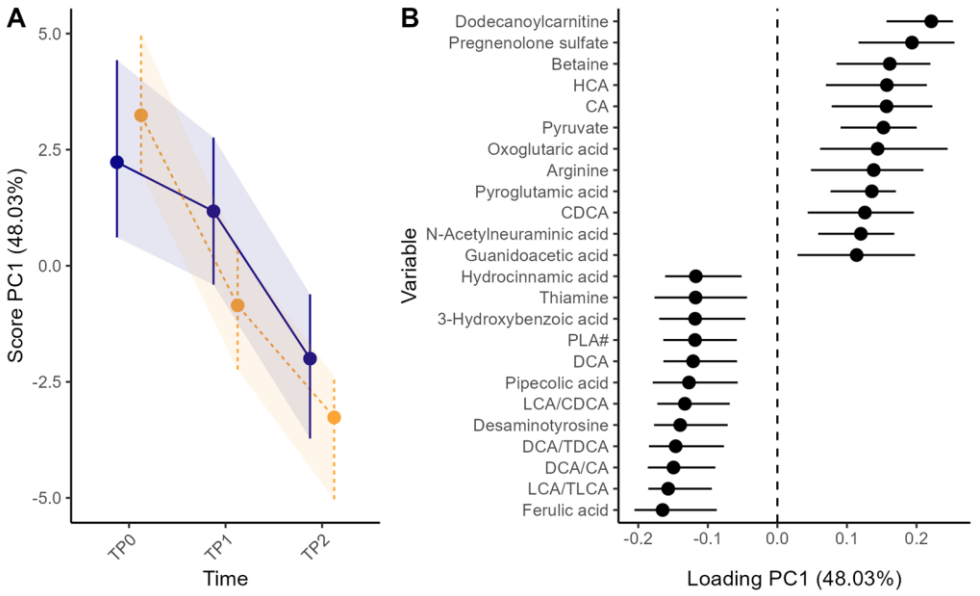

Figure 1. *RM-ASCA+ combined effect matrix showing the common metabolome development throughout the study for the CM-allergic (blue solid line, n=15) and CM-tolerant (orange dashed line, n=24) groups as scores (A) and loadings (B). Only the metabolites with 12 highest and 12 lowest loadings are shown in the plot. Error bars representing 95% CI were estimated based nonparametric bootstrapping.*

Next, the RM-ASCA+ interaction effect matrix was examined to focus on the alterations associated with CM-tolerance acquisition. The PC1 scores and loading of the interaction matrix, **Figure 2**, suggest that compared to the CM-allergic group, the CM-tolerant group showed overall alterations in amino acid metabolism with an increase in citrulline, lysine, N-acetyltyrosine, phenylacetic acid, gamma-aminobutyric acid (GABA#), glutamate, orotate, ornithine and a decrease in 5-hydroxytryptophan and serotonin. The BAs metabolism was also altered: decline in CDCA, CA, glycochenodeoxycholic acid (GCDCA), tauroursodeoxycholic acid (TUDCA), taurochenodeoxycholic acid (TCDCA) and increase in LCA/CDCA for the CM-tolerant group. The BSCFAs, isobutyrate and isovalerate, also contributed to PC1, showing higher levels in the CM-tolerant group. However, only citrulline and lysine were found significantly different at TP2 between the two groups univariately (**Table S6** in Online Supplementary Materials, **Figure S2**).

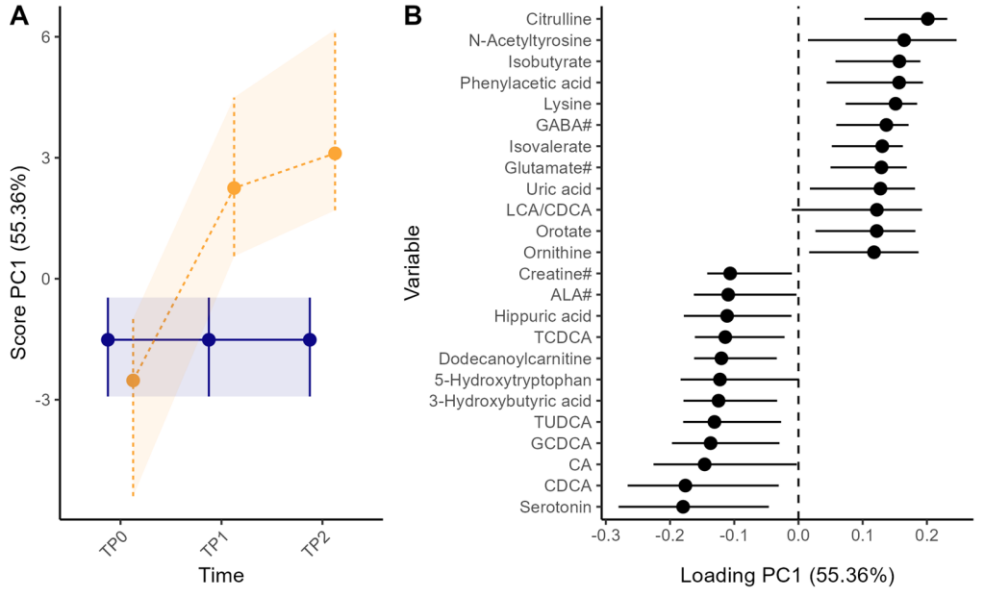

Figure 2. *RM-ASCA+ interaction effect matrix showing the metabolome differences between the CM-allergic (blue solid line, n=15) and CM-tolerant group (orange dashed line, n=24) over time as scores (A) and loadings (B). Only the metabolites with 12 highest and 12 lowest loadings are shown in the plot. Error bars representing 95% CI were estimated based nonparametric bootstrapping.*

3.3 Synbiotic supplementation altered fecal metabolome after six months of intervention

The longitudinal alterations of the fecal metabolome between the AAF and AAF-S group were studied to understand the effect of the synbiotic supplementation. As shown in **Figure 3**, clear group separation was observed in PC1 of the RM-ASCA+ interaction effect matrix, especially at TP1.

Among all the metabolites, 12 metabolites and three BA ratios were found to be statistically different between the AAF and AAF-S groups at TP1, and only inosine at TP2 (**Figure S3**, **Table S2**). The estimated marginal means plot of those analytes can be found in **Figure S3**. The synbiotic supplementation led to an increase of gut microbial metabolites indolelactic acid and 4-hydoxyphenyllactic acid (4-OH-PLA#) and a decline in the fatty acids linoleic acid (LA), alpha-linolenic acid (ALA#), and oleic acid (OA) at TP1 (**Figure 4**). Amino acid glutamine was also decreased in the AAF-S group at TP1. Three purine metabolites inosine, guanine, and adenine as well as the pyrimidine uridine were also affected by the intervention. Although adenine was higher upon the synbiotic addition, the opposite was true for inosine, guanine, and uridine. HCA and CDCA/GCDCA, CA/glycocholic acid (GCA), ursodeoxycholic acid (UDCA)/glycoursodeoxycholic acid (GUDCA) were all significantly higher in the AAF-S than in the AAF group at TP1, whereas GCDCA was significantly lower (**Figure 4**). A few other BAs were found to be among the main contributors to PC1 of the interaction matrix (**Figure 3**) or to have significant interaction coefficient at TP1 before multiple testing correction

(**Figure 4**), namely, the glyco-conjugated BAs GCA and GUDCA and the secondary BAs and their ratio to primary BAs: LCA, DCA, DCA/CA, and LCA/CDCA.

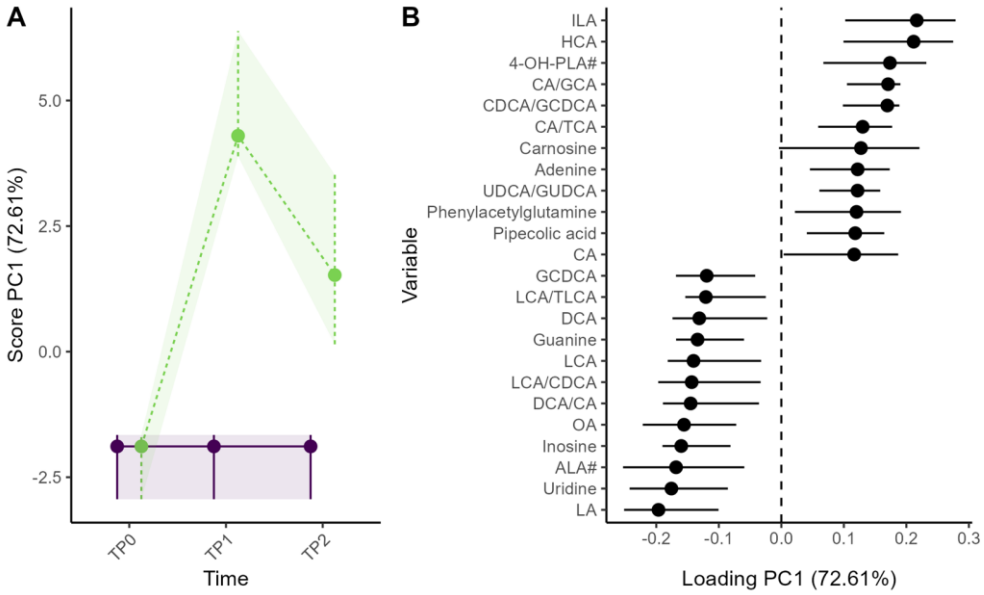

Figure 3. *RM-ASCA+ interaction effect matrix showing the metabolome differences between the AAF (purple solid line, n=16) and AAF-S (green dashed line, n=23) group over time as scores (A) and loadings (B). Only the metabolites with 12 highest and 12 lowest loadings are shown in the plot. Error bars representing 95% CI were estimated based nonparametric bootstrapping.*

3.4 Association between changes in Bifidobacterium and metabolites significantly altered by the synbiotic

The synbiotic supplementation significantly increased the relative abundance of Bifidobacterium in the AAF-S group from baseline to TP1 and TP2 compared to the AAF group (**Figure S4**).[35] To determine whether these increases were associated with the significantly changed metabolites, Spearman's rank correlation analysis was performed between the changes in metabolite levels and Bifidobacterium's relative abundance from baseline to TP1 (TP1-TP0) and TP2 (TP2-TP0), respectively (**Table S3**). In the AAF-S group, changes in ILA and 4-OH-PLA# from TP0 to later time points were positively correlated with those of Bifidobacterium ($r>0.6$, $p<0.005$), while changes in glutamine were negatively correlated ($r\leq-0.5$, $p<0.05$) (**Figure 5**). The changes in Bifidobacterium were positively correlated with those of adenine at TP1 and TP2 in both groups ($r>0.5$, $p<0.05$), and with CDCA/GCDCA and CA/GCA only at TP1 in the AAF-S group ($r>0.4$, $p<0.05$). Bifidobacterium also showed negative correlations with GCDCA and inosine in changes from TP0 to TP1 only in the AAF-S group ($r<-0.4$, $p<0.05$) (**Figure S5**).

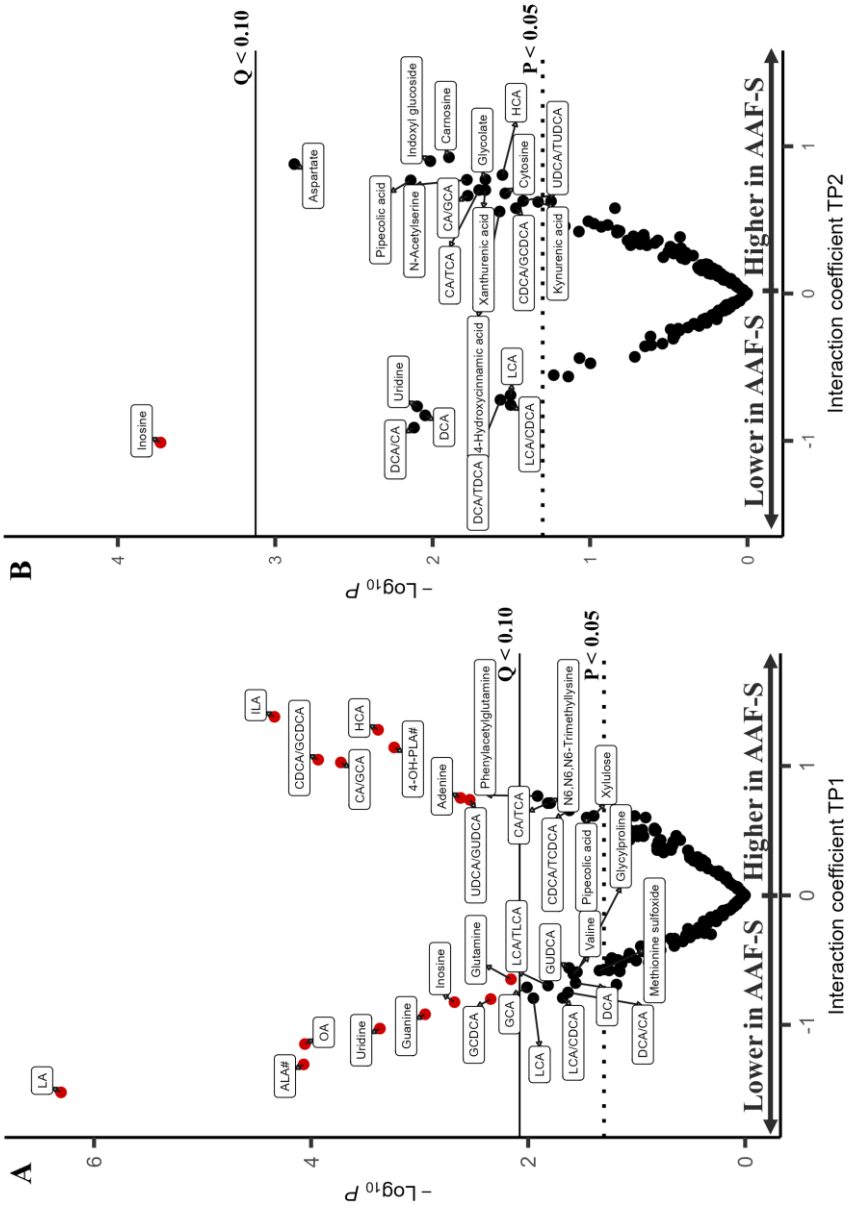

Figure 4. *Volcano plot showing the resulting p-value of the interaction coefficient for TP1 (left) and TP2 (right) in intervention LMM, dashed (p = 0.05), solid line (Q = 0.1) for TP1 (A) and TP2 (B). Red symbols indicate metabolites with Q<0.1 after Benjamini-Hochberg procedure.*

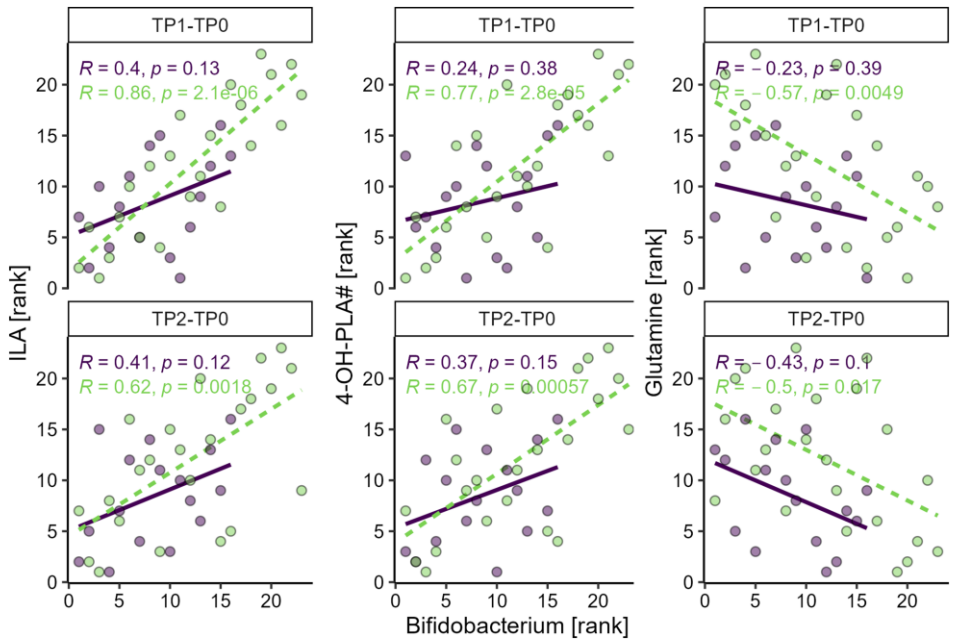

Figure 5. *Spearman's rank correlations between the changes in Bifidobacterium and ILA, 4-OH-PLA#, glutamine in AAF (purple solid line, n=16) and AAF-S (green dashed line, n=23) groups from baseline to TP1 (TP1-TP0) and TP2 (TP2-TP0). The rank of the changes in metabolite response and relative abundance of Bifidobacterium within each group were used for plotting. The figure shows p values; the Q values after Benjamini-Hochberg procedure are provided in Table S3.*

4. Discussion

In this study we followed the fecal metabolome alterations in infants with IgE-mediated CMA who received AAF with or without synbiotics for a year. Firstly, we examined the effect of CM-tolerance acquisition on the fecal metabolome over time. Time, reflecting growth and diet diversification, had a more pronounced impact on the metabolome than CM-tolerance acquisition (**Figure 1**, **Figure S1**). The diet enrichment was evidenced by the overall increase of the phenolic acids which are ubiquitously produced in plants,[37] including ferulic acid, 3-hydroxybenzoic acid, and hydrocinnamic acid. The decrease in the steroid hormone (pregnenolone sulfate), energy metabolites (pyruvate, oxoglutaric acid, and dodecanoylcarnitine), and the altered amino acids and derivatives (pyroglutamic acid, arginine, pipecolic acid) suggest metabolome modification associated with somatic growth.[38,39]

The multivariate RM-ASCA+ analysis showed an association of CM-tolerance acquisition status with alterations in amino acids, BAs, and (B)SCFAs (**Figure 2**). Compared to infants with persistent CMA, citrulline and lysine were significantly higher in the infants who developed CM-tolerance at TP2 (**Figure S2**). Lower plasma citrulline levels are known

marker of increased gut permeability,[40] which can raise the chance of allergen(s) passing the intestinal barrier and triggering the immune system.[41] The increase in fecal citrulline in the CM-tolerant group in this study might suggest improved gut barrier function and gut health. Although not significantly different between the two groups, the amino acids GABA#, glutamate#, threonine#, and ornithine were also higher in the CM-tolerant group compared to the CM-allergic group (**Figures S1-S2**). Lower fecal threonine levels have previously been reported in infants with IgE-mediated CMA compared to healthy controls.[42] Interestingly, although not significant, 5-hydroxytryptophan and serotonin were higher in the CM-allergic group at TP1 and TP2 (**Figure 2**), while their precursor tryptophan significantly declined only from TP0 to TP2 in this group (**Figure S1**). As serotonin is involved in intestinal epithelial proliferation[43] and plays an essential role in regulating intestinal inflammation,[44] the upregulated tryptophan-serotonin metabolism in the CM-allergic group may reflect an inflammatory state of the intestine in the CMA infants.

Children who outgrew CMA showed differences in their BAs profile. The primary BAs (CA, CDCA) significantly decreased, while the secondary BAs (DCA, LCA) and the secondary/primary BAs ratios (DCA/CA, LCA/CDCA) significantly increased from TP0 to TP2 only in the CM-tolerant group (**Figure S1**). A recent study found that, compared to healthy children, children with IgE-mediated CMA had lower ratios of fecal secondary/primary BAs from the CA pathway, with DCA and other oxidized keto BAs included in the calculation.[45] Secondary BAs from the CDCA pathway, including LCA, were reported lower in children with food allergy compared to healthy controls as well.[46] Although the secondary BAs and secondary/primary BAs ratios were not significantly different between the two groups in our study, the altered BAs profiles in the CMA-tolerant group likely indicate a more mature GM for secondary BAs production. This may contribute to improved intestinal functions in infants outgrowing CMA, as LCA is known to attenuate disruption in the intestinal barrier.[47]

(B)SCFAs were also altered during the CMA tolerance acquisition process. Butyrate significantly increased from TP0 to TP2 only in the CM-tolerant group (**Figure S1**). Isobutyrate and isovalerate tended to have group separation at TP1, with a continuous elevation in the CM-tolerant group over time, and a decrease at TP1 in the CM-allergic group (**Figure S2**). Consistent with our finding, those (B)SCFAs, specifically butyrate, are known for their antiinflammatory effects,[27,48] and are generally observed to be lower in feces of children with IgE-mediated food allergy.[42,48] Additionally, phenylalanine, phenyllactic acid (PLA#), and desaminotyrosine, which are GM metabolites from amino acids and dietary polyphenols,[49–51] were significantly increased from TP0 and TP2 only in the CM-tolerant group (**Figure S1**). The significant elevations of these metabolites may promote CM-tolerance acquisition, especially considering the recently recognized antiinflammatory property of desaminotyrosine.[52,53]

The synbiotic (*B. breve* M-16V, FOS: inulin, oligofructose) significantly altered the levels of aromatic lactic acids, purine metabolites as well as fatty acids and BAs, particularly after six months of intervention. The intervention enhanced ILA and 4-OH-PLA levels (**Figure S3**), and

their increases from baseline to TP1 and TP2 were positively correlated with those of bifidobacteria (**Figure 5**). This finding aligns with reports that ILA and 4-OH-PLA are metabolites of tryptophan[29,54,55] and tyrosine[29] produced by infant-type Bifidobacterium species, including *B. breve*. Earlier published microbiome and metaproteomics analysis of stool samples from the same clinical trial revealed that the synbiotic raised the level of bifidobacteria,[19,35] as well as bifidobacterial carbohydrate-active enzymes,[35] known to metabolize FOS.[56] Although the proportion of *Bifidobacterium* was significantly higher in the AAF-S group compared to the AAF group at both time points (**Figure S4**),[19,35] the increases in ILA and 4-OH-PLA# were significantly higher in the AAF-S group only at TP1. These results suggest that the synbiotic promoted the growth and/or the activity of aromatic lactic acids producers, for example, infant-type Bifidobacterium species, especially at TP1. This can be evidenced by stronger positive correlations between changes in the two aromatic lactic acids and bifidobacteria from baseline to TP1 than to TP2 in the AAF-S group (**Figure 5**). To validate our observations, *Bifidobacterium* species should be quantified. Alternatively, aromatic lactate dehydrogenase reported to convert tryptophan and tyrosine to respectively ILA and 4-OH-PLA in infant-type Bifidobacterium species should be analyzed.[29] The possibility that the ILA and 4-OH-PLA# were produced by some lactic acid bacteria should not be ignored either.[57,58] Overall, the increased ILA and 4-OH-PLA# levels in the AAF-S group suggest enhanced abundance or activity of infant-type bifidobacteria, supporting the successful synbiotic supplementation together with the microbiome and metaproteomics findings.[19,35] Although the parent study found that the CM-tolerance acquisition after 12 (TP2) and 24 months of synbiotic intervention aligned with natural outgrowth,[19] our findings, along with the reported antiinflammatory effect of ILA,[25,29,55,59] suggest that the synbiotic intervention may pose beneficial effects on infants' immune system. Further metabolomics studies on larger cohorts are required to verify this hypothesis.

In addition to the increase in ILA and 4-OH-PLA, the synbiotic lowered inosine, guanine, and uridine and raised adenine levels. The same purine-pyrimidine trend was observed in conventionally raised and core microbiota-colonized mice in comparison to germ-free mice,[60] indicating the importance of the GM in purine and pyrimidine metabolism.[60] A decline of inosine and uridine has also been reported in co-culture of *B. breve* with small intestinal-like epithelial cells.[61] *Lactobacillus brevis*, belonging to the *Lactobacillaceae* family, was found to be elevated in the AAF-S group for the same set of samples[35] and was also reported to have inosine degradation capabilities.[62] To link the purine-pyrimidine metabolism to the gut microbiome, and the role of *Bifidobacterium* spp. and *Lactobacillaceae* spp. herein, more research is required.

The AAF-S intervention lowered LA, ALA#, and OA levels, suggesting high consumption of these fatty acids by gut bacteria. This may be a result of hydration by bacteria of the Lactobacillus and Bifidobacterium genera[63] or production of conjugated fatty acids.[64–68]

Bifidobacterium strains, especially *B. breve*, are among the best producers of conjugated linoleic acids[66,67] and conjugated linolenic acids.[66,68]

The synbiotic enhanced the deconjugation of BAs, especially at TP1, where significantly decreased GCDCA and increased CDCA/GCDCA, CA/GCA, and UDCA/GUDCA were observed in the AAF-S compared to AAF group (**Figure 4**). Bifidobacterium, in general, are active bile salt hydrolase (BSH) producers,[69] which perform preferred deconjugation activity on glyco-conjugated BAs.[70] This aligns with our results showing that *Bifidobacterium* changes from baseline correlated negatively with those of GCDCA, and positively with those of CA/GCA and CDCA/GCDCA at TP1 in the AAF-S (**Figure S5**). These correlations in changes disappeared at TP2, possibly due to increased GM diversity. Compared to TP0, families from other phyla, including Bacteroidetes, Firmicutes, and Proteobacteria, were more abundant at later timepoints in both groups, especially at TP2.[35] These bacteria have also been identified as active BSH producers,[71] thus might eliminate the correlation between the activity of BAs deconjugation and Bifidobacterium. Unexpectedly, the increased deconjugation activity of BAs failed to promote the production DCA and LCA. In contrast, although not significant, their levels and ratios to precursors (DCA/CA, LCA/CDCA) were lower in the AAF-S than the AAF group (**Figure 4**). Considering that the conversion of primary BAs to secondary ones is highly conserved in bacteria with the bai operon,[72] and that the host liver can further hydroxylate secondary BAs to tertiary BAs after gut-liver circulation,[73] it is likely that more complex mechanisms underlie the host-gut metabolism of BAs during the intervention.

Our study has several limitations, including the wide age range of the participants at baseline of 3-13 (9.00 ± 2.90) months. Considering the rapid development of the GM in the first two years of life,[39] the wide age range may obscure the observation of fecal metabolome alterations related to CM-tolerance acquisition and the effect of intervention. Another limitation is the lack of information on the CM-tolerance status at TP1. Knowing the status at TP1 could have aided in the interpretation of CM-tolerance acquisition results. The research carried out for this paper is exploratory due to the small samples size (39 subjects). Increasing the sample size is necessary to verify these findings and would also allow to build LMM and RM-ASCA+ models following the intervention and CM-tolerance acquisition simultaneously. In addition, the parent study concluded that the synbiotic supplementation did not significantly affect CMA-resolution. Thus, in this study we cannot draw any conclusions regarding the clinical benefits of the synbiotic supplementation on CM-tolerance acquisition based on fecal metabolome alterations. Despite those limitations, our study revealed several fecal metabolome pathway alterations which may contribute to CMA outgrowth. Most importantly, we found that the AAF-S significantly altered the fecal metabolome after six months of the intervention, not after 12 months, suggesting that early intervention is required to maximize the effect of synbiotics. These findings aid in understanding the link between IgE-mediated CMA-tolerance acquisition, GM, and synbiotics intervention.

Author contributions

M.V.S: Conceptualization, Investigation, Methodology, Formal Analysis, Visualization, Data curation, Writing – Original Draft Preparation; **P.Z.**: Conceptualization, Investigation, Methodology, Writing – Review & Editing; **A.K.**: Conceptualization, Supervision, Writing – Review & Editing; **The TEMPO study team**: Resources; **H.W.**: Conceptualization, Writing – review and editing **C.B.**: Conceptualization, Funding acquisition, Writing – review and editing; **A.C.H.**: Conceptualization, Supervision, Writing – Review & Editing; T.H.: Conceptualization, Supervision, Funding acquisition, Writing – review & editing.

Acknowledgments

This study was part of the EARLYFIT project (Partnership programme NWO Domain AES-Danone Research & Innovation), funded by the Dutch Research Council (NWO) and Danone Research & Innovation (project number: 16490). Pingping Zhu Would like to acknowledge the China Scholarship Council (CSC, No. 201906240049). Diana M Hendrickx (Wageningen University) is gratefully acknowledged for providing the processed 16S rRNA sequencing data. Pascal Mass (Leiden University) is greatly appreciated for his invaluable assistance in metabolomics data pre-processing. We also thank Jolanda Lambert (Danone Research & Innovation) for project management, Guus Roeselers (Danone Research & Innovation) for his input in the study design, and Simone Eussen (Danone Research & Innovation) for her valuable feedback in manuscript review.

Conflict of interest statement

Harm Wopereis is an employee of Danone Research & Innovation. The project is part of a partnership programme between NWO-TTW and Danone Research & Innovation. The other authors declare that they have no known conflicts of interest.

Data Availability Statement

The data that support the findings of this study are openly available in MetaboLights at **www.ebi.ac.uk/metabolights/**, reference number MTBLS12775.

References

1. Sicherer, S. H. & Sampson, H. A. Food allergy. Journal of Allergy and Clinical Immunology 125, S116–S125 (2010).
2. Savage, J. & Johns, C. B. Food Allergy: Epidemiology and Natural History. Immunol Allergy Clin North Am 35, 45–59 (2015).
3. Flom, J. D. & Sicherer, S. H. Epidemiology of Cow's Milk Allergy. Nutrients 11, 1051 (2019).
4. Høst, A. Frequency of cow's milk allergy in childhood. Annals of Allergy, Asthma & Immunology 89, 33–37 (2002).
5. Schoemaker, A. A. et al. Incidence and natural history of challenge-proven cow's milk allergy in European children – EuroPrevall birth cohort. Allergy 70, 963–972 (2015).

6. Johansson, S. G. O. et al. Revised nomenclature for allergy for global use: Report of the Nomenclature Review Committee of the World Allergy Organization, October 2003. Journal of Allergy and Clinical Immunology 113, 832–836 (2004).
7. Saarinen, K. M., Pelkonen, A. S., Mäkelä, M. J. & Savilahti, E. Clinical course and prognosis of cow's milk allergy are dependent on milk-specific IgE status. Journal of Allergy and Clinical Immunology 116, 869–875 (2005).
8. Skripak, J. M., Matsui, E. C., Mudd, K. & Wood, R. A. The natural history of IgE-mediated cow's milk allergy. Journal of Allergy and Clinical Immunology 120, 1172–1177 (2007).
9. Savova, M. V. et al. Current insights into cow's milk allergy in children: Microbiome, metabolome, and immune response—A systematic review. Pediatric Allergy and Immunology 35, e14084 (2024).
10. Turroni, F. et al. Bifidobacteria and the infant gut: an example of co-evolution and natural selection. Cell. Mol. Life Sci. 75, 103–118 (2018).
11. Kumar, H. et al. The Bifidogenic Effect Revisited—Ecology and Health Perspectives of Bifidobacterial Colonization in Early Life. Microorganisms 8, 1855 (2020).
12. Saturio, S. et al. Role of Bifidobacteria on Infant Health. Microorganisms 9, 2415 (2021).
13. Davis, J. C. C. et al. Identification of Oligosaccharides in Feces of Breast-fed Infants and Their Correlation with the Gut Microbial Community. Molecular & Cellular Proteomics 15, 2987–3002 (2016).
14. Ioannou, A., Knol, J. & Belzer, C. Microbial Glycoside Hydrolases in the First Year of Life: An Analysis Review on Their Presence and Importance in Infant Gut. Frontiers in Microbiology 12, (2021).
15. Vandenplas, Y. et al. Current Guidelines and Future Strategies for the Management of Cow's Milk Allergy. JAA Volume 14, 1243–1256 (2021).
16. Vandenplas, Y., Greef, E. D. & Veereman, G. Prebiotics in infant formula. Gut Microbes 5, 681–687 (2014).
17. Jing, W., Liu, Q. & Wang, W. Bifidobacterium bifidum TMC3115 ameliorates milk protein allergy in by affecting gut microbiota: A randomized double-blind control trial. Journal of Food Biochemistry 44, e13489 (2020).
18. Mennini, M. et al. Gut Microbiota Profile in Children with IgE-Mediated Cow's Milk Allergy and Cow's Milk Sensitization and Probiotic Intestinal Persistence Evaluation. International Journal of Molecular Sciences Article (2021).
19. Chatchatee, P. et al. Tolerance development in cow's milk–allergic infants receiving amino acid–based formula: A randomized controlled trial. Journal of Allergy and Clinical Immunology 149, 650-658.e5 (2022).
20. Viljanen, M. et al. Probiotic effects on faecal inflammatory markers and on faecal IgA in food allergic atopic eczema/dermatitis syndrome infants. Pediatr Allergy Immunol 16, 65–71 (2005).
21. Burks, A. W. et al. Synbiotics-supplemented amino acid-based formula supports adequate growth in cow's milk allergic infants. Pediatric Allergy and Immunology 26, 316–322 (2015).
22. Verma, R. et al. Cell surface polysaccharides of Bifidobacterium bifidum induce the generation of Foxp3 + regulatory T cells. Sci. Immunol. 3, eaat6975 (2018).
23. Ruohtula, T. et al. Maturation of Gut Microbiota and Circulating Regulatory T Cells and Development of IgE Sensitization in Early Life. Frontiers in Immunology 10, (2019).
24. Cukrowska, B., Bierła, J. B., Zakrzewska, M., Klukowski, M. & Maciorkowska, E. The Relationship between the Infant Gut Microbiota and Allergy. The Role of Bifidobacterium breve and Prebiotic Oligosaccharides in the Activation of Anti-Allergic Mechanisms in Early Life. Nutrients 12, 946 (2020).
25. Henrick, B. M. et al. Bifidobacteria-mediated immune system imprinting early in life. Cell 184, 3884-3898.e11 (2021).

26. Belenguer, A. et al. Two Routes of Metabolic Cross-Feeding between Bifidobacterium adolescentis and Butyrate-Producing Anaerobes from the Human Gut. Appl Environ Microbiol 72, 3593–3599 (2006).
27. Siddiqui, M. T. & Cresci, G. A. The Immunomodulatory Functions of Butyrate. JIR Volume 14, 6025–6041 (2021).
28. Acevedo, N. et al. Perinatal and Early-Life Nutrition, Epigenetics, and Allergy. Nutrients 13, 724 (2021).
29. Laursen, M. F. et al. Bifidobacterium species associated with breastfeeding produce aromatic lactic acids in the infant gut. Nat Microbiol 6, 1367–1382 (2021).
30. Hendrickx, D. M. et al. Assessment of infant outgrowth of cow's milk allergy in relation to the faecal microbiome and metaproteome. Sci Rep 13, 12029 (2023).
31. Wopereis, H. et al. Intestinal microbiota in infants at high risk for allergy: Effects of prebiotics and role in eczema development. Journal of Allergy and Clinical Immunology 141, 1334-1342.e5 (2018).
32. Hosseinkhani, F., Dubbelman, A.-C., Karu, N., Harms, A. C. & Hankemeier, T. Towards Standards for Human Fecal Sample Preparation in Targeted and Untargeted LC-HRMS Studies. Metabolites 11, 364 (2021).
33. Zhu, P. et al. Development of an Untargeted LC-MS Metabolomics Method with Postcolumn Infusion for Matrix Effect Monitoring in Plasma and Feces. J. Am. Soc. Mass Spectrom. 35, 590–602 (2024).
34. Wei, R. et al. Missing Value Imputation Approach for Mass Spectrometry-based Metabolomics Data. Sci Rep 8, 663 (2018).
35. Hendrickx, D. M. et al. Trackability of proteins from probiotic Bifidobacterium spp. in the gut using metaproteomics. Beneficial Microbes 14, 269–280 (2023).
36. Jarmund, A. H., Madssen, T. S. & Giskeødegård, G. F. ALASCA: An R package for longitudinal and cross-sectional analysis of multivariate data by ASCA-based methods. Frontiers in Molecular Biosciences 9, (2022).
37. Heleno, S. A., Martins, A., Queiroz, M. J. R. P. & Ferreira, I. C. F. R. Bioactivity of phenolic acids: Metabolites versus parent compounds: A review. Food Chemistry 173, 501–513 (2015).
38. De Peretti, E. & Mappus, E. Pattern of Plasma Pregnenolone Sulfate Levels in Humans from Birth to Adulthood. The Journal of Clinical Endocrinology & Metabolism 57, 550–556 (1983).
39. Holzhausen, E. A. et al. Longitudinal profiles of the fecal metabolome during the first 2 years of life. Sci Rep 13, 1886 (2023).
40. Fragkos, K. C. & Forbes, A. Citrulline as a marker of intestinal function and absorption in clinical settings: A systematic review and meta-analysis. United European Gastroenterol J 6, 181–191 (2018).
41. Niewiem, M. & Grzybowska-Chlebowczyk, U. Intestinal Barrier Permeability in Allergic Diseases. Nutrients 14, 1893 (2022).
42. Francavilla, R. et al. Effect of lactose on gut microbiota and metabolome of infants with cow's milk allergy. Pediatric Allergy and Immunology 23, 420–427 (2012).
43. Shah, P. A., Park, C. J., Shaughnessy, M. P. & Cowles, R. A. Serotonin as a Mitogen in the Gastrointestinal Tract: Revisiting a Familiar Molecule in a New Role. Cellular and Molecular Gastroenterology and Hepatology 12, 1093–1104 (2021).
44. Haq, S., Grondin, J. A. & Khan, W. I. Tryptophan-derived serotonin-kynurenine balance in immune activation and intestinal inflammation. The FASEB Journal 35, e21888 (2021).
45. De Paepe, E. et al. Integrated gut metabolome and microbiome fingerprinting reveals that dysbiosis precedes allergic inflammation in IgE-mediated pediatric cow's milk allergy. Allergy 79, 949–963 (2024).
46. Lee, S.-Y. et al. The alternative bile acid pathway can predict food allergy persistence in early childhood. Pediatric Allergy and Immunology 34, e14003 (2023).

47. Calzadilla, N. et al. Bile acids as inflammatory mediators and modulators of intestinal permeability. Front. Immunol. 13, 1021924 (2022).
48. De Paepe, E., Van Gijseghem, L., De Spiegeleer, M., Cox, E. & Vanhaecke, L. A Systematic Review of Metabolic Alterations Underlying IgE-Mediated Food Allergy in Children. Molecular Nutrition & Food Research 65, 2100536 (2021).
49. Beloborodov, N. V., Khodakova, A. S., Bairamov, I. T. & Olenin, A. Yu. Microbial origin of phenylcarboxylic acids in the human body. Biochemistry Moscow 74, 1350–1355 (2009).
50. Rechner, A. Colonic metabolism of dietary polyphenols: influence of structure on microbial fermentation products. Free Radical Biology and Medicine 36, 212–225 (2004).
51. Schoefer, L., Mohan, R., Schwiertz, A., Braune, A. & Blaut, M. Anaerobic Degradation of Flavonoids by Clostridium orbiscindens. Appl Environ Microbiol 69, 5849–5854 (2003).
52. Wei, Y. et al. The intestinal microbial metabolite desaminotyrosine is an anti-inflammatory molecule that modulates local and systemic immune homeostasis. The FASEB Journal 34, 16117–16128 (2020).
53. Steed, A. L. et al. The microbial metabolite desaminotyrosine protects from influenza through type I interferon. Science 357, 498–502 (2017).
54. Sakurai, T., Odamaki, T. & Xiao, J. Production of Indole-3-Lactic Acid by Bifidobacterium Strains Isolated fromHuman Infants. Microorganisms 7, 340 (2019).
55. Ehrlich, A. M. et al. Indole-3-lactic acid associated with Bifidobacterium-dominated microbiota significantly decreases inflammation in intestinal epithelial cells. BMC Microbiol 20, 357 (2020).
56. Tanno, H. et al. Characterization of fructooligosaccharide metabolism and fructooligosaccharide-degrading enzymes in human commensal butyrate producers. Gut Microbes 13, 1–20 (2021).
57. Valerio, F., Lavermicocca, P., Pascale, M. & Visconti, A. Production of phenyllactic acid by lactic acid bacteria: an approach to the selection of strains contributing to food quality and preservation. FEMS Microbiology Letters 233, 289–295 (2004).
58. Pan, T. et al. Uncovering the specificity and predictability of tryptophan metabolism in lactic acid bacteria with genomics and metabolomics. Front. Cell. Infect. Microbiol. 13, (2023).
59. Meng, D. et al. Indole-3-lactic acid, a metabolite of tryptophan, secreted by Bifidobacterium longum subspecies infantis is anti-inflammatory in the immature intestine. Pediatr Res 88, 209–217 (2020).
60. Kasahara, K. et al. Gut bacterial metabolism contributes to host global purine homeostasis. Cell Host Microbe 31, 1038-1053.e10 (2023).
61. Sen, A. et al. Comprehensive analysis of metabolites produced by co-cultivation of Bifidobacterium breve MCC1274 with human iPS-derived intestinal epithelial cells. Front. Microbiol. 14, (2023).
62. Wang, H. et al. Lactobacillus brevis DM9218 ameliorates fructose-induced hyperuricemia through inosine degradation and manipulation of intestinal dysbiosis. Nutrition 62, 63–73 (2019).
63. Serra, S., De Simeis, D., Castagna, A. & Valentino, M. The Fatty-Acid Hydratase Activity of the Most Common Probiotic Microorganisms. Catalysts 10, 154 (2020).
64. Alonso, L., Cuesta, E. P. & Gilliland, S. E. Production of Free Conjugated Linoleic Acid by Lactobacillus acidophilus and Lactobacillus casei of Human Intestinal Origin1. Journal of Dairy Science 86, 1941–1946 (2003).
65. Salsinha, A. S., Pimentel, L. L., Fontes, A. L., Gomes, A. M. & Rodríguez-Alcalá, L. M. Microbial Production of Conjugated Linoleic Acid and Conjugated Linolenic Acid Relies on a Multienzymatic System. Microbiology and Molecular Biology Reviews 82, 10–1128 (2018).
66. Gorissen, L. et al. Production of conjugated linoleic acid and conjugated linolenic acid isomers by Bifidobacterium species. Appl Microbiol Biotechnol 87, 2257–2266 (2010).

67. Mei, Y. et al. Research progress on conjugated linoleic acid bio-conversion in Bifidobacterium. International Journal of Food Microbiology 369, 109593 (2022).
68. Park, H. G. et al. Production of a Conjugated Fatty Acid by Bifidobacterium breve LMC520 from α-Linolenic Acid: Conjugated Linolenic Acid (CLnA). J. Agric. Food Chem. 60, 3204–3210 (2012).
69. Tanaka, H., Doesburg, K., Iwasaki, T. & Mierau, I. Screening of Lactic Acid Bacteria for Bile Salt Hydrolase Activity. Journal of Dairy Science 82, 2530–2535 (1999).
70. Kim, G.-B., Yi, S.-H. & Lee, B. H. Purification and Characterization of Three Different Types of Bile Salt Hydrolases from Bifidobacterium Strains. Journal of Dairy Science 87, 258–266 (2004).
71. Song, Z. et al. Taxonomic profiling and populational patterns of bacterial bile salt hydrolase (BSH) genes based on worldwide human gut microbiome. Microbiome 7, 9 (2019).
72. Guzior, D. V. & Quinn, R. A. Review: microbial transformations of human bile acids. Microbiome 9, 140 (2021).
73. Zhang, J. et al. Continuum of Host-Gut Microbial Co-metabolism: Host CYP3A4/3A7 are Responsible for Tertiary Oxidations of Deoxycholate Species. Drug Metab Dispos 47, 283–294 (2019).

Supplementary Materials

Online Supplementary Materials are available in the original manuscript:
DOI: 10.1002/mnfr.202400583

Chemicals

Methyl tert-butyl ether (MTBE, ≥99.8%) and ammonium formate (≥99.0%) were purchased from Sigma Aldrich (St. Louis, United States). LC-MS-grade methanol (MeOH), isopropanol and formic acid (FA) were purchased from Biosolve B.V. (Valkenswaard, Netherlands). LC-MS grade acetonitrile was purchased from Actu-all chemicals (Randmeer, The Netherlands) and Biosolve B.V. (Valkenswaard, Netherlacnjugnds). Purified water was obtained from a Milli-Q PF Plus system (Merck Millipore, Burlington, United States). List of the isotopically labelled standards (SILs), including supplier details, can be found in **Table S1** in Online Supplementary Materials.

Sample preparation

Briefly, 72 µL of water and 216 µL MeOH, containing stable isotopically labelled standards (SILs) (**Table S1** in Online Supplementary Materials), were added to the 20 mg dry-weight fecal sample. After a 3-minute vortex mixing (Marshall Scientific, Cambridge, UK) 120 µL ice-cold MTBE was added, followed by another 3-minute vortex mixing. Following a brief centrifugation (30s, 100g, 4 °C), 200 µL of water and 168 µL of MTBE were added. The samples were vortex mixed for another 3 min, incubated at 4°C for 10 minutes until centrifugation (20 min, 16 000g, 4°C) inducing aqueous and organic layer separation. All solvents used during the LLE were ice-cold and vortex mixing was always at maximum speed. Following layer separation, each layer was transferred to an Eppendorf tube, followed by 5 and 2.5 minutes of centrifugation (16000g, 4°C) for aqueous and organic layers respectively. After extraction, 150 µL of the aqueous layer was aliquoted for polar to semi-polar metabolites analysis, while 48.8 µL of aqueous and 28.8 µL of organic layer was combined for the bile and fatty acids analysis. The aliquots were dried in a Speedvac (Labcono, USA) and stored at -80°C. Prior to LC-MS analysis, the extracts were reconstituted in 50 µL of 0.1% FA in water for polar to semi-polar metabolites analysis, and 200 µL of MeOH for the bile and fatty acids analysis. The reconstitution solvents contained different SILs (**Table S1** in Online Supplementary Materials).

Quality Control

Samples were randomized into two batches, with those from the same subject prepared and measured in the same batch. For the preparation of the quality control sample, 30 study samples were weighed and extracted. After the extraction, equal volumes of each layer were taken from each sample and pooled, resulting in pooled QC aqueous and organic layers. Those pooled layers were used to prepare QC samples for each platform. The LLE and aliquoting steps were performed as described in Sample preparation.

LC-MS analysis of polar to semi polar metabolites

Analysis of polar to semi-polar metabolites was performed on a UPLC-TOF/MS system consisting of a Shimadzu LC system coupled to a TripleTOF 6600 mass spectrometer (SCIEX, Foster City, CA, USA) with an electrospray ionization source (ESI) that operated at both positive and negative ion modes. The ESI source parameters were set as follows: spray voltage ±4.5 kV, capillary temperature 400 ◦C, sheath gas 40, auxiliary gas 40, curtain gas 45. Data were acquired under full scan mode over the m/z range of 60-800 Da. The LC separation was carried out at 40 °C using a Waters Acquity UPLC HSS T3 column (1.8 µm, 2.1 mm × 100 mm) with pre-column in-line stainless steel filter (0.3 µm, Agilent Technologies, Waldbronn, Germany). The mobile phase A was 0.1% FA in water, and the mobile phase B was 0.1% FA in ACN (Actu-all chemicals). With a flow rate of 0.4 mL min-1 and 1 µL of injection volume, the gradient starts at 100% A; 0–0.5 min 80% A; 0.5–2.5 min 2% A; 2.5–7.5 min 2% A; 7.5–12 min 2% A; 12 – 15 100% A. The data were acquired under full scan mode over the m/z range of 60-800 Da with Analyst TF software 1.7.1 (SCIEX) in negative and positive ionization modes. The preferred ionization mode for metabolites detectable in both polarities was chosen based on lower RSD% and higher signal-to-noise ratio of the QC samples.

LC-MS analysis of bile acid and fatty acids

Analysis of bile and fatty acids was performed on an UPLC-TOF/MS system consisting of ExionLC™ AC UHPLC system and SCIEX ZenoTOF 7600 system (Darmstadt, Germany) equipped with an IonDrive™ Turbo V Source, operated in negative ESI mode. The ion source conditions were as follows: spray voltage of 4.5 kV, capillary temperature of 550°C, ion source gas 1 50 psi, ion source gas 2 50 psi, curtain gas 35 psi, CAD gas 7 psi. The MS data was acquired under full scan mode over the m/z range of 200-900 Da. Accumulation time was set to 0.25 s, delustering potential to -70V and collision energy to -10eV. Chromatographic separation was performed on a Waters Acquity UPLC HSS T3 column (1.8 µm, 2.1 mm × 100 mm) with pre-column in-line stainless steel filter (0.3 µm, Agilent Technologies, Waldbronn, Germany). The flow rate was set at 0.4 ml min-1, the column was kept at 45 °C, injection volume at 2 µL. Mobile phase A consisted of 10 mM ammonium formate in water/ACN (Biosolve B.V) (95:5, v:v), while mobile phase B was 10 mM ammonium formate in MeOH/water (99:1, v:v). The gradient was as follows: starting at 0% B; 0–0.2 min 70% B; 0.2–7.5 min 100% B; 7.5–11.5 min 100% B; 11.5–11.6 min 0% B; 11.6 – 15 0% B. Isopropanol was used as an external rinsing solution (2 s sip time + rinse port). The flow was directed to waste in the first minute of the run. The autosampler temperature was set at 10 °C. Data acquisition was carried out on SCIEX OS 2.1.6.

Visualization RM-ASCA+

Visualization of the longitudinal metabolomic alterations was achieved using RM-ASCA+, which is an extension of LMMs for multivariate data. In the first step, LMMs are used to decompose the response matrix into effect matrices. The effect matrices are then analyzed

using principal component analysis (PCA), and the results are summarized into PCA scores and loadings. The LMMs used for RM-ASCA+ were the LMMs used for the univariate analysis. The visualized effect matrices included the time effect matrix ('time') which shows time development of the reference group over time. The interaction matrix ('time:group') and the group-interaction matrix ('group + time:group') both show the deviations of the study group compared to the reference group over time with the latter also displaying the baseline differences. Lastly, the combined matrix ('time + time:group' or 'time + group + time:group') shows the time development of both the study and the reference group.

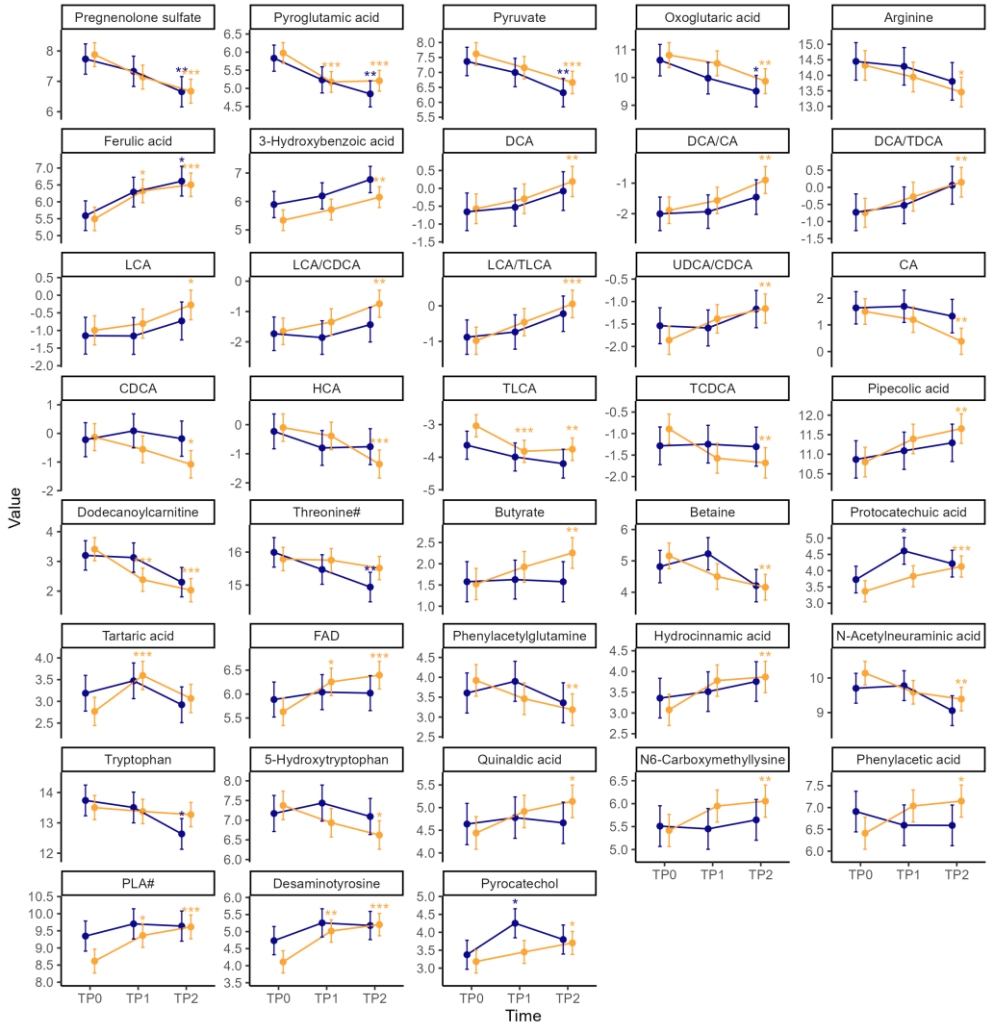

Figure S1. *Marginal means estimated from the LMMs for participants who acquired tolerance (CM-tolerant, orange) and those that remained allergic (CM-allergic, blue). Only the metabolites for which pairwise comparison in time was found significant are plotted. The q-values are based on the marginal mean comparison to TP0 for each group, q < 0.01 (***), q < 0.05 (**), q <0.1 (*).*

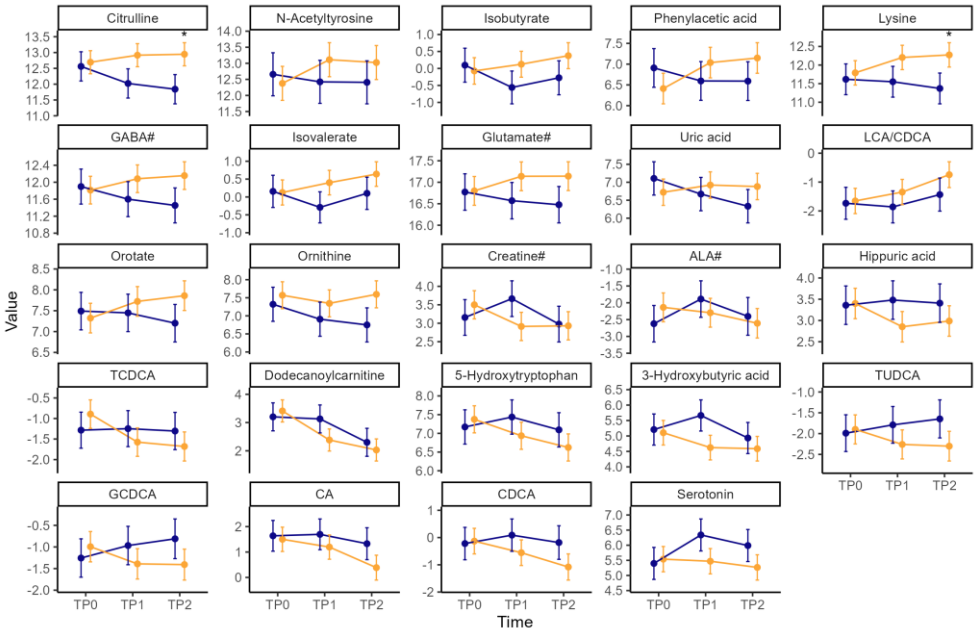

Figure S2. *Marginal means estimated from the LMMs for participants who acquired tolerance (CM-tolerant, orange) and those that remained allergic (CM-allergic, blue). The metabolites with top loadings in PC1 of the RM-ASCA+ interaction matrix are plotted. The q-values are based on the marginal mean comparison between the groups at each time point, q <0.1 (*).*

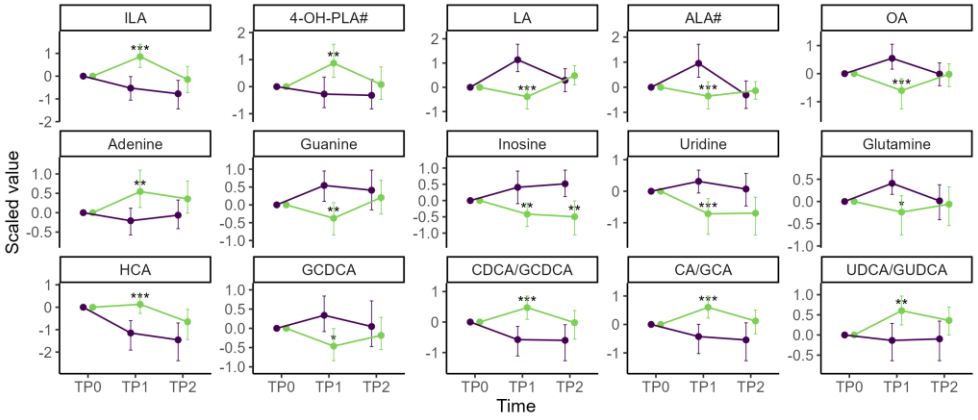

Figure S3. *Marginal means estimated from the LMMs for AAF (purple) and AAF-S (green) group. Only the metabolites for which an interaction coefficient was found significant are plotted. The response has been scaled. The q-values are based on/denote the significant between-group change in the within-group change from baseline. q < 0.01 (***), q < 0.05 (**), q <0.1 (*)*

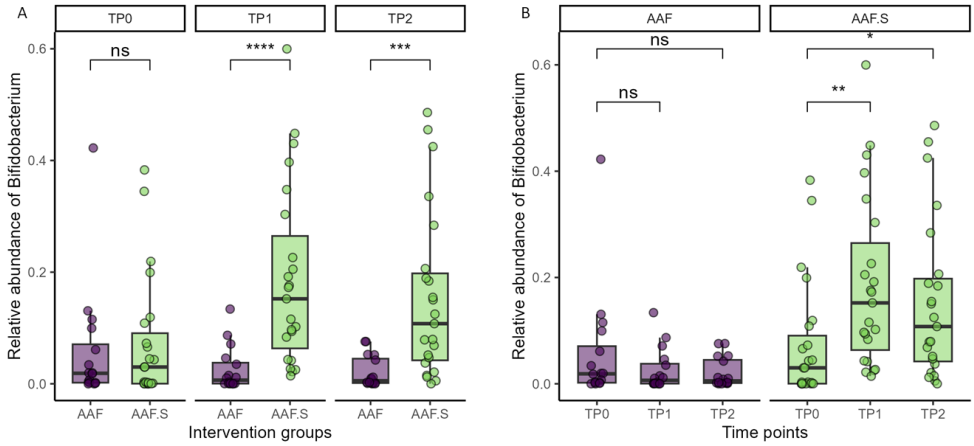

Figure S4. *Relative abundance of Bifidobacterium comparisons between AAF and AAF-S groups at each time point (A), and between time points in each group (B). Statistical significance was evaluated with two-side unpaired t-tests; p > 0.05 (ns), p ≤ 0.05 (*), p ≤ 0.01 (**), p ≤ 0.001 (***), p ≤ 0.0001 (****).*

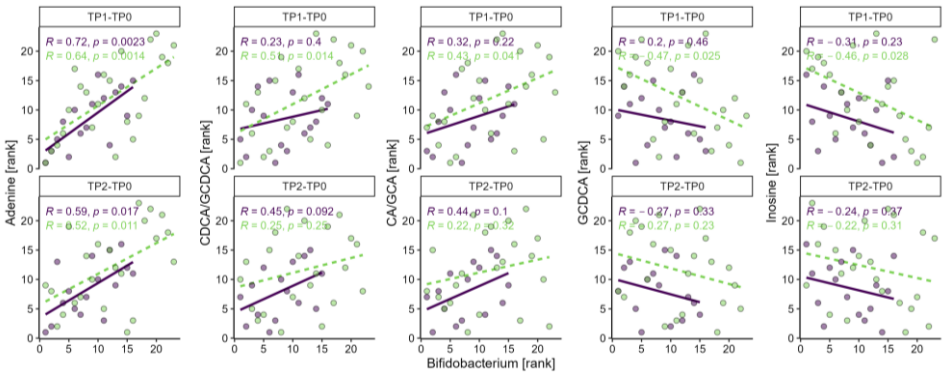

Figure S5. *Spearman's rank correlations between the changes in Bifidobacterium and adenine, CDCA/GCDCA, CA/GCA. GCDCA, inosine in AAF (purple solid line) and AAF-S (green dashed line) groups from baseline to TP1 (TP1-TP0) and TP2 (TP2-TP0). The rank of the changes in metabolite response and relative abundance of Bifidobacterium within each group were used for plotting.*

Table S1. Abbreviations of target analytes. A name or abbreviation followed by "#" indicates coelution with other targets.

Compound name	Abbreviations
Dihydrocaffeic acid/3-hydroxy-3-(3-hydroxyphenyl)propanoic acid/Hydroxyphenyllactic acid	4-OH-PLA#
3-Methylxanthine/1-Methylxanthine/ 7-Methylxanthine	Methylxanthine isomers
Phenyllactic acid/3-(3-Hydroxyphenyl)propanoic acid	PLA#
p-Hydroxyphenylacetic acid/Mandelic acid	p-Hydroxyphenylacetic acid#
alpha-Aminobutyric acid/gamma-Aminobutyric acid/3-Aminoisobutanoic acid/Dimethylglycine	GABA#
Indolelactic acid	ILA
myo-Inositol/ Galactose/ Fructose	Fructose#
O-Acetylserine/Glutamic acid	Glutamate#
1-Methyladenosine/N6-Methyladenosine/2'-O-Methyladenosine	1-Methyladenosine#
5-Aminolevulinic acid/4-Hydroxyproline	5-Aminolevulinic acid#
Adenosine/Deoxyguanosine	Adenosine#
Alanine/beta-Alanine/Sarcosine	Alanine#
Creatine/Beta-Guanidinopropionic acid	Creatine#
Cytidine	Cytidine
Targinine/Homoarginine	Homoarginine#
N1-Methyl-4-pyridone-3-carboxamide/Nudifloramide	Nudifloramide#
Symmetric dimethylarginine/Asymmetric dimethylarginine	SDMA#
Threonine/Homoserine	Threonine#
Cholic acid	CA
Chenodeoxycholic acid	CDCA
Deoxycholic acid	DCA
Oleic acid	OA
Linoleic acid	LA
alpha-Linolenic acid/gamma-Linolenic acid	ALA#
Dihomo-gamma-linolenic acid/Dihomo-alpha-linolenic acid	DGLA
Arachidonic acid	AA
Eicosapentaenoic acid	EPA
4,8,12,15,19-Docosapentaenoic acid	DPA
Docosahexaenoic acid	DHA
Glycocholic acid	GCA
Glycochenodeoxycholic acid	GCDCA
Glycoursodeoxycholic acid	GUDCA
Hyocholic acid	HCA
Lithocholic acid	LCA
Taurocholic acid	TCA
Taurochenodesoxycholic acid	TCDCA
Taurodeoxycholic acid	TDCA
Tauroursodeoxycholic acid	TUDCA
Taurolithocholic acid	TLCA
Ursodeoxycholic acid	UDCA

Table S2. Significantly altered metabolites in CM-allergic and CM-tolerant groups from marginal means comparison

CM-Allergic				
Metabolite	TP0	TP1	P value	Q value
Protocatechuic acid	3.727 (3.317, 4.137)	4.607 (4.197, 5.017)	0.0006	0.0674
Pyrocatechol	3.374 (2.969, 3.778)	4.252 (3.847, 4.656)	0.0008	0.0674
CM-Allergic				
Metabolite	TP0	TP2	P value	Q value
Pyroglutamic acid	5.833 (5.472, 6.194)	4.849 (4.489, 5.21)	0.0002	0.0328
Threonine#	15.992 (15.544, 16.44)	14.939 (14.491, 15.387)	0.0004	0.0340
Pyruvic acid	7.365 (6.89, 7.841)	6.322 (5.847, 6.798)	0.0006	0.0347
Pregnenolone sulfate	7.735 (7.236, 8.234)	6.658 (6.159, 7.157)	0.0011	0.0460
Tryptophan	13.74 (13.233, 14.247)	12.636 (12.129, 13.142)	0.0030	0.0806
Oxoglutaric acid	10.624 (10.057, 11.191)	9.508 (8.941, 10.076)	0.0033	0.0806
Ferulic acid	5.59 (5.151, 6.029)	6.61 (6.171, 7.049)	0.0034	0.0806
CM-Tolerant				
Metabolite	TP0	TP1	P	Q
Tartaric acid	2.769 (2.443, 3.094)	3.597 (3.271, 3.922)	0.0001	0.0082
Pyroglutamic acid	5.977 (5.691, 6.262)	5.178 (4.893, 5.463)	0.0001	0.0082
Dodecanoylcarnitine	3.411 (3.02, 3.802)	2.383 (1.992, 2.774)	0.0002	0.0082
TLCA	-3.038 (-3.378, -2.698)	-3.819 (-4.159, -3.479)	0.0002	0.0082
Desaminotyrosine	4.112 (3.785, 4.44)	5.017 (4.689, 5.344)	0.0003	0.0095
Ferulic acid	5.495 (5.148, 5.842)	6.323 (5.976, 6.67)	0.0026	0.0707
PLA#	8.617 (8.268, 8.965)	9.364 (9.015, 9.712)	0.0042	0.0920
FAD	5.631 (5.342, 5.92)	6.255 (5.966, 6.544)	0.0044	0.0920
Pregnenolone sulfate	7.88 (7.486, 8.275)	7.141 (6.746, 7.535)	0.0051	0.0945
CM-Tolerant				
Metabolite	TP0	TP2	P	Q
Dodecanoylcarnitine	3.411 (3.02, 3.802)	2.03 (1.639, 2.421)	6.10E-07	0.0001
Pregnenolone sulfate	7.88 (7.486, 8.275)	6.675 (6.281, 7.07)	3.88E-06	0.0003
Desaminotyrosine	4.112 (3.785, 4.44)	5.204 (4.877, 5.532)	1.22E-05	0.0007
LCA/TLCA	-0.98 (-1.363, -0.598)	0.054 (-0.335, 0.443)	0.0001	0.0025
Pyruvate	7.619 (7.243, 7.995)	6.664 (6.288, 7.04)	0.0001	0.0025
PLA#	8.617 (8.268, 8.965)	9.615 (9.267, 9.963)	0.0001	0.0030
Protocatechuic acid	3.367 (3.043, 3.691)	4.128 (3.804, 4.452)	0.0002	0.0040
HCA	-0.1 (-0.574, 0.373)	-1.354 (-1.836, -0.871)	0.0002	0.0040
Ferulic acid	5.495 (5.148, 5.842)	6.505 (6.158, 6.852)	0.0002	0.0040
Pyroglutamic acid	5.977 (5.691, 6.262)	5.21 (4.924, 5.495)	0.0002	0.0043
FAD	5.631 (5.342, 5.92)	6.396 (6.107, 6.685)	0.0004	0.0064
TLCA	-3.038 (-3.378, -2.698)	-3.756 (-4.101, -3.41)	0.0008	0.0113
Pipecolic acid	10.801 (10.423, 11.178)	11.656 (11.279, 12.034)	0.0010	0.0141
DCA/CA	-1.888 (-2.322, -1.454)	-0.899 (-1.341, -0.456)	0.0015	0.0188
Oxoglutaric acid	10.807 (10.359, 11.256)	9.865 (9.417, 10.314)	0.0016	0.0188
DCA/TDCA	-0.745 (-1.17, -0.321)	0.149 (-0.283, 0.582)	0.0019	0.0209
3-Hydroxybenzoic acid	5.341 (4.976, 5.706)	6.151 (5.786, 6.516)	0.0023	0.0234
Betaine	5.159 (4.751, 5.567)	4.16 (3.752, 4.568)	0.0027	0.0262
TCDCA	-0.893 (-1.24, -0.547)	-1.681 (-2.035, -1.327)	0.0030	0.0278
N-Acetylneuraminic acid	10.142 (9.802, 10.483)	9.392 (9.051, 9.732)	0.0032	0.0279
CA	1.501 (1.022, 1.979)	0.386 (-0.104, 0.875)	0.0040	0.0327
Hydrocinnamic acid	3.076 (2.698, 3.454)	3.869 (3.491, 4.246)	0.0041	0.0327
UDCA/CDCA	-1.858 (-2.175, -1.542)	-1.156 (-1.479, -0.832)	0.0054	0.0392

CM-Tolerant				
Metabolite	TP0	TP2	P	Q
LCA/CDCA	-1.654 (-2.092, -1.216)	-0.744 (-1.191, -0.297)	0.0054	0.0392
Butyrate	1.522 (1.153, 1.891)	2.255 (1.893, 2.617)	0.0055	0.0392
Phenylacetylglutamine	3.922 (3.524, 4.321)	3.185 (2.786, 3.583)	0.0073	0.0481
DCA	-0.571 (-0.988, -0.155)	0.192 (-0.232, 0.616)	0.0076	0.0481
N6-Carboxymethyllysine	5.415 (5.064, 5.767)	6.055 (5.704, 6.406)	0.0076	0.0481
5-Hydroxytryptophan	7.375 (7.013, 7.737)	6.623 (6.261, 6.985)	0.0131	0.0802
CDCA	-0.131 (-0.601, 0.339)	-1.081 (-1.561, -0.601)	0.0139	0.0809
Quinaldic acid	4.44 (4.08, 4.8)	5.138 (4.777, 5.498)	0.015	0.08089
Arginine	14.321 (13.842, 14.799)	13.461 (12.983, 13.94)	0.015	0.08089
Pyrocatechol	3.184 (2.864, 3.504)	3.703 (3.383, 4.023)	0.015	0.08089
Phenylacetic acid	6.412 (6.044, 6.78)	7.148 (6.78, 7.516)	0.016	0.08089
LCA	-0.995 (-1.408, -0.583)	-0.276 (-0.696, 0.145)	0.016	0.08089
TP2				
Metabolite	Allergic	Tolerant	P value	Q value
Citrulline	11.841 (11.378, 12.303)	12.946 (12.58, 13.311)	0.0003	0.0537
Lysine	11.371 (10.957, 11.785)	12.273 (11.946, 12.601)	0.0010	0.0823

Table S3. Spearman's rank correlation between the changes of bifidobacterium and metabolites/ratios which are significantly altered in the AAF-S group. Only correlations significant following multiple testing correlation are displayed

Compound	Rho	P value	Time points	Intervention	Q value
ILA	0.859	2.13E-06	TP1-TP0	AAF-S	<2.00E-04
4-OH-PLA#	0.769	2.81E-05	TP1-TP0	AAF-S	2.00E-04
Adenine	0.637	0.00138	TP1-TP0	AAF-S	0.0069
Glutamine	-0.573	0.0049397	TP1-TP0	AAF-S	0.0185
Adenine	0.721	0.0023058	TP1-TP0	AAF	0.0346
CDCA/GCDCA	0.508	0.0144412	TP1-TP0	AAF-S	0.0433
Inosine	-0.462	0.0275279	TP1-TP0	AAF-S	0.059
GCDCA	-0.468	0.0254131	TP1-TP0	AAF-S	0.059
CA/GCA	0.431	0.0413402	TP1-TP0	AAF-S	0.0775